

Fluid modeling of laser-driven implosion of magnetized spherical targets

S. Atzeni¹, F. Barbato¹, A. Forte^{1,2}

¹ *Dipartimento SBAI, Università di Roma “La Sapienza”, Roma, Italy*

² *Department of Physics, University of Oxford, Oxford, UK*

1. Introduction

Magnetic fields of the order of hundred of MG (10 kT) may relax ignition conditions for inertial confinement fusion (ICF) [1]. The nearly axial magnetic field generated by one or two coils can be strongly compressed in the laser-driven implosion of a spherical target, and increased neutron production has been reported [2, 3]. Recently, experiments on magnetized exploding pushers were performed [4]. Magnetized targets are also envisaged for fast ignition [5].

Such developments motivate the present work. We have upgraded our 2-D Lagrangian ICF code DUED [6, 7] by including models for magnetic field evolution and for the effects of the field on plasma and charged fusion product transport. In the following we outline the model and its solution, and present preliminary applications of the code.

2. Extended-MHD DUED code

An initially axial magnetic field \mathbf{B} (as in the experiments of Refs. [2, 3, 4]) is easily dealt with using the DUED code cylindrical r - z scheme. Subsequent evolution of \mathbf{B} leads to the generation of out-of-plane components. For the moment, we neglect such components, which are relatively small in many cases of interest. We can therefore use a 2-D model also for the magnetic field. By proceeding similarly to Ref. [8], we write an equation for the evolution of \mathbf{B} . Rather than solving the equations for the two components of \mathbf{B} , we solve the equation for azimuthal component of the vector potential A_ϕ . In the DUED lagrangian framework such an equation reads

$$\frac{dA_\phi}{dt} = -\frac{u_r}{r}A_\phi + \frac{\eta_\perp}{\mu_0} \left[\nabla^2 A_\phi - \frac{A_\phi}{r^2} \right] - \left[v_{Nz} \frac{\partial A_\phi}{\partial z} + v_{Nr} \frac{\partial A_\phi}{\partial r} + v_{Nr} \frac{A_\phi}{r} \right], \quad (1)$$

where u_r is the r component of the fluid velocity, η_\perp is the resistivity in direction orthogonal to \mathbf{B} , \mathbf{v}_N is the Nernst velocity, which we compute as $\mathbf{v}_N = -k_\perp \nabla T_e / 2.5 p_e$ (see, e.g. [8]), with k_\perp the perpendicular electron conductivity, T_e the electron temperature and p_e the electron pressure. The first term on the r.h.s. of Eq. (1) describes advection of \mathbf{B} (frozen-in-flow), the second one the diffusion of \mathbf{B} , and the third the Nernst effect.

The finite-differenced version of Eq. (1) is solved efficiently by a fractional step procedure, dealing sequentially with advection, diffusion, and Nernst term. Treatment of the advection term is trivial and exact (as the Lagrangian mesh just moves with the fluid). The diffusive contribution

is dealt with an appropriately modified version of the standard Kershaw's scheme [9] already used by DUED for all diffusive equations. Finally, the Nernst term is differenced with a sort of 2-D Lax-Wendroff method or, alternatively, with a 2-D upwind method. Details on the schemes as well as on the implementation of the boundary conditions will be given elsewhere. A flux-limiter has to be applied to the Nernst velocity (just as to thermal conductivity).

We then obtain \mathbf{B} from $\mathbf{B} = \nabla \times \mathbf{A}$. The $\mathbf{j} \times \mathbf{B} = \nabla \mathbf{B} \times \mathbf{B} / \mu_0$ force term and ohmic heating are included in the momentum equation and the electron energy equation, respectively. Transport coefficients of the magnetized plasma are computed using the fits by Epperlein and Haines [10]. (However, no significant differences are observed using the coefficients by Braginskii [11].)

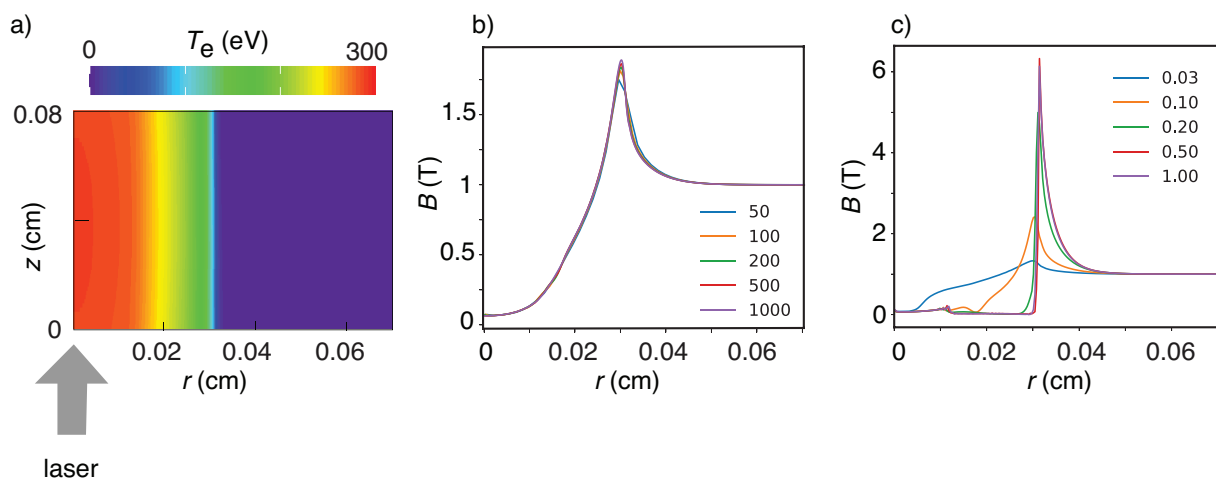


Figure 1: Test problem to validate Nernst term treatment: laser heated low density gas, with parameters as in Sec. II of Ref. [12] and initial uniform magnetic of 1 T (along z). a) Electron temperature map at the end of the laser pulse ($t = 0.5$ ns); b) radial profiles of magnetic field at $z = 0.04$ cm, for different radial meshing and the same Nernst flux limiter $f_N = 0.07$; the curve labels indicate the number of radial mesh points N_r ; c) same as b), but for different values of f_N (labeling the curves), and for $N_r = 200$

Validation of the advection and diffusive terms was straightforward. For the Nernst term, instead, there are neither standard benchmarks nor experimental data. However, we ran a problem proposed in Ref. [12] [see Fig. 1a]): a low density deuterium plasma, immersed in a uniform magnetic field of 1 T, is irradiated by a moderate intensity laser beam with gaussian radial intensity profile, propagating in the direction of the magnetic field. The laser heats the plasma to about 300 eV and the magnetic field is expelled from the central hot plasma, due to Nernst effect. DUED results are practically independent of mesh spacing [Fig. 1b)] and also on the finite-differencing scheme used for the Nernst term (upwind or Lax-Wendroff). Instead, the profile of the magnetic field depends strongly on the Nernst flux-limiter [Fig. 1c)].

3. Magnetized target implosion

We discuss here an application of DUEED to the simulation of magnetized targets. We refer to the experimental parameters reported in Refs. [2, 3, 8], namely a CH shell with outer radius of $430\ \mu\text{m}$ and thickness of $27\ \mu\text{m}$, filled with D_2 gas at density of about $1.6\ \text{mg}/\text{cm}^3$. The target is irradiated by a $1\ \text{ns}$ laser pulse with wavelength of $350\ \text{nm}$ and flat-top power of $18\ \text{TW}$. The implosion stagnates around $t = 2\ \text{ns}$. Shell convergence is about 20. Experiments were performed both with unmagnetized targets and with targets imbedded in a field of $8\ \text{T}$ ($80\ \text{kG}$). The simulations show that the initial magnetic field is strongly compressed, up to more than $5\ \text{KT}$ in a small portion of the hot stagnating gas. However, the distribution of the magnetic field depends critically on the value of Nernst flux limiter, and further studies are required on this issue.

Concerning the fusion yield, it is well known that fluid codes over-predict the yield of the above implosions. However, concerning yield enhancement due to magnetization, DUEED preliminary results indicate enhancements up to about 20%, as experimentally observed. Again, results depend significantly on the Nernst flux limiter, and additional investigations are in progress.

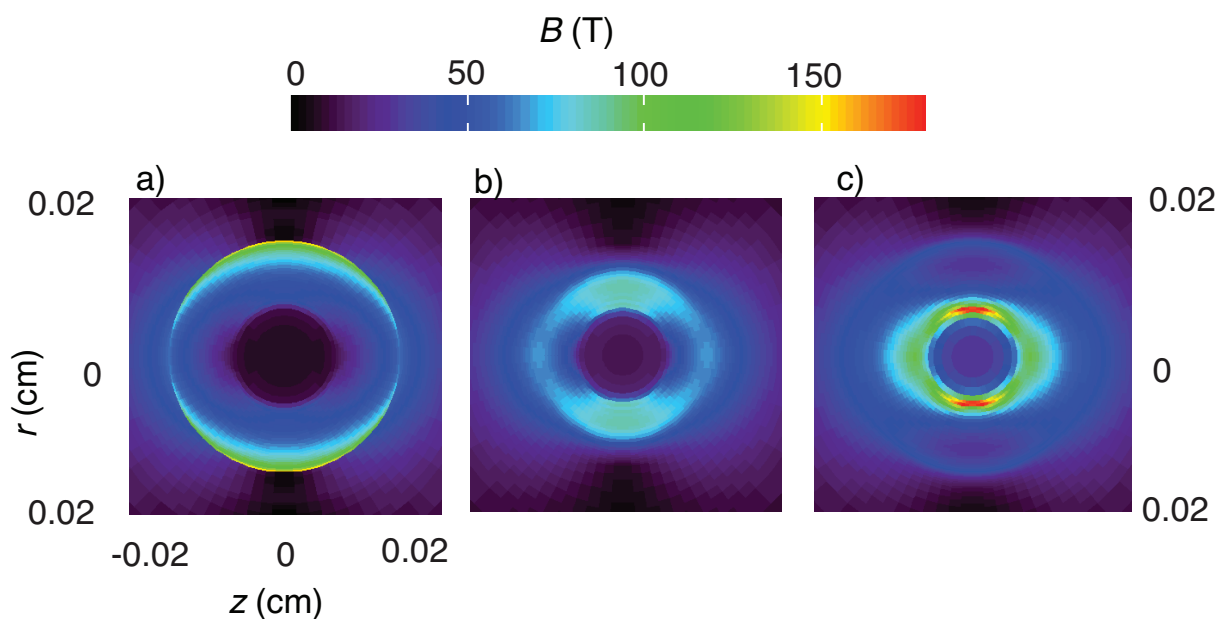


Figure 2: Maps of the intensity of the magnetic field during the implosion (instantaneous convergence about 4) from simulations with a) field advection only; b) advection and diffusion; c) advection, diffusion and Nernst effect.

The early and intermediate stages of the implosion seem to be less sensitive to modeling uncertainties, and simulations clearly illustrate the effect of the various terms contributing to

magnetic field evolution. For instance, Fig. 2 shows maps of the intensity of the magnetic field at time $t \simeq 1.5$ ns, when the shell has converged by a factor about 4. The three frames of the figure refer to simulations with a) advection only (frozen-in law); b) advection and diffusion; c) advection, diffusion and electrothermal (Nernst) effect (with both electron conductivity flux limiter and Nernst flux limiter of 0.07).

Systematic studies of this target and of magnetized exploding pushers are programmed for the near future. We also plan to investigate the effect on magnetic fields of hot-spot ignited inertially confined fuels.

This work has been carried out within the framework of the EUROfusion Enabling research projects AWP19-20-ENR-IFE19.CEA-01 and AWP21-ENR-01-CEA-02, and has received funding from the Euratom research and training programme 2019-2020 and 2021-2025 under grant no. 633053. The views and opinions expressed herein do not necessarily reflect those of the European Commission. We thank A. Bose, J. R. Davies (LLE, Rochester) A. Schiavi (Roma Sapienza) and C. A. Walsh (LLNL) for useful discussions.

References

- [1] L. J. Perkins *et al.*, Phys. Plasmas **20**, 072708 (2013); *ibidem* **24**, 062708 (2017)
- [2] P.-Y. Chang *et al.*, Phys. Rev. Lett. **107**, 135006 (2011)
- [3] M. Hohenbeger *et al.*, Phys. Plasmas **19**, 056306 (2012)
- [4] A. Bose *et al.*, 61st APS-DPP (2019): meetings.aps.org/link/BAPS.2019.DPP.CO8.6
- [5] S. Sakata *et al.*, Nature Commun. **9**, 2238 (2018)
- [6] S. Atzeni, Comput. Phys. Commun **43**, 107 (1986)
- [7] S. Atzeni *et al.*, Comput. Phys. Commun. **169**, 153 (2005)
- [8] J. R. Davies *et al.*, Phys. Plasmas **22**, 112703 (2015)
- [9] D. S. Kershaw, J. Comp. Phys. **39**, 375 (1981)
- [10] E. M. Epperlein and M. G. Haines, Phys. Fluids **29** 1063 (1986)
- [11] S. I. Braginskii, "Transport processes in a plasma", Reviews Plasma Physics, Vol. 1, (Consultants Bureau, NY, 1965)
- [12] C. A. Walsh *et al.*, Phys. Plasmas **27**, 022103 (2020)